In situ IR, Raman, and UV-Vis DRS spectroscopy of supported vanadium oxide catalysts during methanol oxidation

Loyd J. Burcham [a], Goutam Deo [b], Xingtao Gao [a] and Israel E. Wachs [a,*]

[a] *Zettlemoyer Center for Surface Studies and Department of Chemical Engineering, Lehigh University, Bethlehem, PA 18015, USA*
[b] *Department of Chemical Engineering, Indian Institute of Technology, Kanpur 208-016, UP, India*

The application of *in situ* Raman, IR, and UV-Vis DRS spectroscopies during steady-state methanol oxidation has demonstrated that the molecular structures of surface vanadium oxide species supported on metal oxides are very sensitive to the coordination and H-bonding effects of adsorbed methoxy surface species. Specifically, a decrease in the intensity of spectral bands associated with the fully oxidized surface (V^{5+}) vanadia active phase occurred in all three studied spectroscopies during methanol oxidation. The terminal V=O ($\sim$1030 cm^{-1}) and bridging V–O–V ($\sim$900–940 cm^{-1}) vibrational bands also shifted toward lower frequency, while the *in situ* UV-Vis DRS spectra exhibited shifts in the surface V^{5+} LMCT band (>25,000 cm^{-1}) to higher edge energies. The magnitude of these distortions correlates with the concentration of adsorbed methoxy intermediates and is most severe at lower temperatures and higher methanol partial pressures, where the surface methoxy concentrations are greatest. Conversely, spectral changes caused by actual reductions in surface vanadia (V^{5+}) species to reduced phases (V^{3+}/V^{4+}) would have been more severe at higher temperatures. Moreover, the catalyst (vanadia/silica) exhibiting the greatest shift in UV-Vis DRS edge energy did not exhibit any bands from reduced V^{3+}/V^{4+} phases in the d–d transition region (10,000–30,000 cm^{-1}), even though d–d transitions were detected in vanadia/alumina and vanadia/zirconia catalysts. Therefore, V^{5+} spectral signals are generally not representative of the percent vanadia reduction during the methanol oxidation redox cycle, although estimates made from the high temperature, low methoxy surface coverage IR spectra suggest that the catalyst surfaces remain mostly oxidized during steady-state methanol oxidation (15–25% vanadia reduction). Finally, adsorbed surface methoxy intermediate species were easily detected with *in situ* IR spectroscopy during methanol oxidation in the C–H stretching region (2800–3000 cm^{-1}) for all studied catalysts, the vibrations occurring at different frequencies depending on the specific metal oxide upon which they chemisorb. However, methoxy bands were only found in a few cases using *in situ* Raman spectroscopy due to the sensitivity of the Raman scattering cross-sections to the specific substrate onto which the surface methoxy species are adsorbed.

Keywords: *in situ* spectroscopy, methanol oxidation, oxide catalysts, vanadia, Raman, infrared, UV-Vis

1. Introduction

The molecular structures of supported metal oxide catalysts have been the subject of intense scrutiny in recent years [1–32], but the states of these structures under *in situ* reaction conditions have received comparably less attention [1,9–17]. Supported metal oxide catalysts consist of a two-dimensional, active surface metal oxide phase that is fully dispersed and chemisorbed onto the surfaces of high surface area oxide supports (e.g., alumina, titania, silica, etc.). Vibrational spectroscopies such as Raman and infrared (IR) have often been used to probe the molecular structures of supported metal oxides, and an especially large amount of information has been obtained for the supported vanadia systems [4,12–32]. These spectroscopies, especially Raman, can detect surface VO_x structures because the underlying oxide support signals are generally weak in the wavenumber regions of interest [1]. In addition, ultraviolet-visible diffuse reflectance spectroscopy (UV-Vis DRS) can provide information about the reduced states of supported vanadia, which do not give rise to detectable IR or Raman signals. However, the majority of these characterization studies have focused on the molecular structures of supported vanadia under static conditions (i.e., fully oxidized or pre-reduced). Therefore, in the present investigation all three of these techniques (Raman, IR, and UV-Vis DRS) are employed under *in situ* reaction conditions to obtain information about the molecular structures of supported vanadia catalysts while methanol oxidation is actually occurring on the catalyst surface.

The molecular structures of the surface vanadia species on calcined, dehydrated catalysts have been shown to consist of VO_4 units possessing a single V=O (mono-oxo) terminal bond, three bridging V–O–M bonds (M = V or support cation), and vanadium atoms in the fully-oxidized, 5+ oxidation state after calcination [1–4,12–32]. These species exhibit a very strong Raman band at $\sim$1030 cm^{-1} ($\pm$3 cm^{-1}, except for the vanadia/silica band at $\sim$1038 cm^{-1}) that shifts slightly with changes in surface vanadia coverage and choice of support. This distinctive Raman band is assigned to the symmetric stretching mode of the terminal V=O bond in the surface vanadia species. At higher loadings of vanadia, another broader and weaker band appears around 900–940 cm^{-1} and is assigned to polymerized V–O–V stretching modes. Additionally, using the V=O stretching frequencies and the bond length correlation developed by Hardcastle and Wachs [1,28] for vanadia compounds, it was calculated that there are only very small differences in the bond lengths of the terminal V=O bond on the various oxide supports ($\pm$0.01 Å across CeO_2, ZrO_2, TiO_2, Nb_2O_5, and Al_2O_3). The den-

* To whom correspondence should be addressed.

sity of active surface vanadia sites is also the same on all of the supports at monolayer coverage (~8 V atoms/nm^2), where monolayer coverage is defined as the highest vanadia loading that produces only surface VO_4 species and not spectrally distinct V_2O_5 microcrystallites as measured by Raman spectroscopy. Specific monolayer coverages on the various oxide supports correspond to ~3 wt% vanadia on ceria (36 m^2/g, 5.7 V atoms/nm^2), ~4% on zirconia (39 m^2/g, 6.8 V atoms/nm^2), ~5% on titania (55 m^2/g, 7.9 V atoms/nm^2), ~7% on niobia (55 m^2/g, 8.4 V atoms/nm^2), and either ~20 or ~25% on alumina depending on the alumina surface area (180 or 250 m^2/g, 7.3 V atoms/nm^2) [1,20,21]. Therefore, the molecular structures of the surface vanadia species are essentially independent of the oxide supports in their calcined, fresh state.

However, vandia supported on silica has been more difficult to disperse at high loadings due to the relatively chemically inert silica surface. Previously, only about 3 wt% V_2O_5/SiO_2 was achievable before forming V_2O_5 microcrystallites [1,20,21]. However, Gao et al. [30] recently prepared highly dispersed V_2O_5/SiO_2 using new synthesis methods. They reached much higher coverage (2.6 V atoms/nm^2 or 12 wt% V_2O_5 on 300 m^2/g SiO_2) and found VO_4 coordination at all loadings based on XANES measurements, consistent with vanadia structures on the other supports. Furthermore, the Raman spectra again exhibited a strong band due to a terminal V=O bond at 1038 cm^{-1}, but no bridging V–O–V mode was found in the ~940 cm^{-1} region. The isolated nature of the surface vanadia species on silica at all loadings is unique to the silica support and has also been observed for other surface metal oxides on silica [1,3,31]. Nevertheless, the isolated VO_4 species on silica has essentially the same molecular structure as the isolated vanadia species at low loadings on the other supports, except that the terminal V=O bond is somewhat shorter for vanadia/silica (higher Raman stretching frequency).

The relationship between these fresh, calcined molecular structures and their catalytic activity has been previously investigated using the methanol oxidation reaction. In particular, fixed-bed reactor studies of supported vanadia monolayer catalysts have indicated a strong support effect upon the turnover frequency (TOF) of the methanol oxidation reaction [3,12,20,21]. The TOF over supported vanadia catalysts is defined as the number of methanol molecules converted to formaldehyde per surface V atom per second. At steady state, the TOFs for supported vanadia catalysts at monolayer coverages (except for submonolayer 3% V_2O_5/SiO_2) under 6% methanol were found to decrease in the following order [20,21], according to support: V_2O_5/CeO_2 (1.0×10^0 s^{-1}), V_2O_5/ZrO_2 (1.7×10^{-1} s^{-1}), V_2O_5/TiO_2 (1.1×10^{-1} s^{-1}), V_2O_5/Nb_2O_5 (4.0×10^{-2} s^{-1}), V_2O_5/Al_2O_3 (6.8×10^{-3} s^{-1}), and V_2O_5/SiO_2 (2.3×10^{-4} s^{-1}). Such a strong support effect has been interpreted as an indication that the bridging V–O–support bonds must be the active centers in the rate-determining step during methanol oxidation, since the terminal V=O Raman band positions and VO_4 coordination are essentially identical on all of the oxide supports [3,12,20,21]. The electronegativity of the oxide support cation in the V–O–support bond has also been correlated to the TOF [20], the more electropositive support cations yielding the higher TOF values.

However, these studies have not been able to determine whether the number of V–O–support bonds involved during reaction (i.e., the steady-state percent V^{5+} reduction) or the activity per V–O–support site is the primary structural factor responsible for the support effect. For example, the oxide supports with surface vanadia species that produce higher apparent TOFs may allow more of the available surface vanadia active sites to participate in the steady-state redox cycle compared to less active supported vanadia catalysts. Alternatively, if the number of vanadia sites (per surface area) that are reduced during steady-state methanol oxidation is constant for vanadia on the various supports, then the intrinsic activity of the individual vanadia sites must be responsible for the support effect. In the present study, the use of *in situ* Raman, IR, and UV-Vis DRS spectroscopies during methanol oxidation will attempt to clarify this issue by examining the surface vanadia species directly during methanol oxidation. These spectroscopies will also be assessed for their ability in detecting *in situ*, steady-state concentrations of adsorbed methoxy (–OCH_3) species, which are the most abundant reactive intermediates during methanol oxidation over oxide catalysts [32,33].

2. Experimental

2.1. Sample preparation

The oxide supports used for the preparation of supported vanadium oxide catalysts were TiO_2 (50 m^2/g, Degussa), ZrO_2 (39 m^2/g, Degussa), CeO_2 (36 m^2/g, Engelhard), Nb_2O_5 (55 m^2/g, Niobium Products Company), $A1_2O_3$ (180 m^2/g, Harshaw, or 250 m^2/g, Engelhard), and SiO_2 (300 m^2/g, Cabot). The vanadium oxide precursor used for this study was vanadium tri-isopropoxide (Alfa, 95–98% purity) and the method used for the preparation was incipient wetness impregnation. The moisture and air sensitive nature of this precursor required that the preparation be performed in a nitrogen environment using non-aqueous solvents. Known amounts of the precursor and methanol (Fisher-certified ACS, 99.9% pure), corresponding to incipient wetness impregnation volume and final amount of vanadium oxide required, were prepared in the glove box filled with nitrogen, mixed thoroughly with the oxide support, and allowed to stand for 16 h. This was followed by various heat treatments in nitrogen (100 °C and 300 °C) prior to the final calcination, which was performed at 450 °C in air for all of the supported vanadium oxide catalysts.

2.2. In situ spectroscopies

The requirements for *in situ* spectroscopy using Raman, IR, and UV-Vis DRS vary significantly between the three quite different techniques, and generally demands modification of the *in situ* experimental conditions and procedures between techniques. These necessary changes in conditions are documented below, and, when relevant, will be incorporated in the interpretation of spectra considered in section 4.

2.2.1. In situ Raman spectroscopy

The laser Raman spectra were obtained with an Ar^+ laser (Spectra Physics, model 165). The incident laser was tuned to 514.5 nm and delivered 50–100 mW of power, measured at the sample. The scattered radiation from the sample was collected at right angles to the laser beam and directed into an OMA Ill (Princeton Applied Research, model 1463 optical multichannel analyzer) with a photodiode array detector thermoelectrically cooled to $-35\,^{\circ}C$. About 100–200 mg of the pure catalyst were pressed into wafers and placed in an *in situ* cell that contained a rotating mount, thermocouple probe, and inlet and outlet gas connections. The arrangement of the *in situ* cell has been outlined elsewhere [31]. To obtain the Raman spectra under dehydrated conditions, the *in situ* cell was heated to $350\,^{\circ}C$ for 1/2 h to desorb the surface moisture and then cooled to room temperature to enhance the signal. The entire procedure was performed in a stream of flowing oxygen (Linde Speciality Grade, 99.99% purity, 100 ml/min). The Raman spectra of the catalysts were also obtained under ambient conditions and checked for the effect of hydration–dehydration and consequently compound formation (the spectra of bulk compounds being unaffected by the presence of adsorbed surface moisture [34]). No compound formation was observed for any of the samples.

In situ Raman spectroscopy for the methanol oxidation reaction was performed at various temperatures (30, 230, 300, and $360\,^{\circ}C$) on the supported vanadium oxide catalysts. The fresh catalyst was dehydrated *in situ* in an O_2 stream (Linde Speciality Grade, 99.99% purity, 100 ml/min) at $400\,^{\circ}C$ for 1 h and then cooled to the reaction temperature. The gas stream was then switched to a stream (100 ml/min) of $CH_3OH/O_2/He$ gas mixture in the molar ratio of 4/20/76. The catalyst was allowed to equilibrate in the reaction stream for 1/2 h before the spectra were collected. Also, to compensate for the experimental fluctuations inherent in the collection of scattered Raman radiation, the spectra were normalized based on the support bands for TiO_2-, ZrO_2-, Nb_2O_5-, and SiO_2-supported vanadium oxide catalysts. For the $A1_2O_3$-supported vanadium oxide catalysts the spectra were normalized based on the 992 cm^{-1} Raman band of crystalline V_2O_5, which was observed not to change during methanol oxidation over the 7% V_2O_5/TiO_2 catalyst. The 7% V_2O_5/TiO_2 catalyst contained vanadium oxide as molecularly dispersed and crystalline V_2O_5 species. The entire dehydration–reduction–reoxidation reaction procedure was performed *in situ* without ever exposing the sample to ambient conditions.

2.2.2. In situ IR spectroscopy

The *in situ* infrared experiments were performed with a BioRad FTS-40A FTIR spectrometer equipped with a DTGS detector. The infrared spectra were recorded at a resolution of 2 cm^{-1} using 250 signal-averaged scans and, after acquisition, were smoothed using the Savitsky–Golay method. Unlike Raman, which is a scattering experiment, the IR was operated in transmission mode using very thin wafers placed in specially designed *in situ* cells. Most of the samples studied with IR (vanadia on TiO_2, CeO_2, Al_2O_3, and SiO_2, as well as the pure supports) were pressed into thin disks of perforated stainless steel (30% open area and ~5–30 mg of catalyst). These wafers were then sealed with stainless steel gaskets inside an *in situ* IR cell of fixed-bed configuration. Exceptions include the V_2O_5/ZrO_2 and pure ZrO_2 samples, which were pressed as self-supporting wafers (~30–60 mg) and placed inside a low-dead volume *in situ* cell of more traditional design. The details of these cell designs are given elsewhere [35].

The following *in situ* experimental procedure was employed. The samples were heated *in situ* to $350\,^{\circ}C$ in a flowing stream (15 ml/min) of oxygen and helium (both ultrahigh purity; JWS technologies) with an O_2/He molar ratio of 25/75. The pretreated catalysts were then cooled to $100\,^{\circ}C$ and methanol was introduced using a pre-mixed gas mixture of $CH_3OH/O_2/He$ (Scott Specialty Gas Co., molar ratio of 0.2/19.8/80) at a flowrate of ~25 ml/min. The low concentration of gas-phase methanol (2000 ppm or 0.2%) was necessary in order to reduce gas-phase methanol signals in the *in situ* IR spectra. The temperature was then slowly ramped to various temperatures up to $300\,^{\circ}C$ under the $CH_3OH/O_2/He$ flow. IR spectra were obtained at each temperature after the signals had reached stable, steady-state values (~10 min), and the methanol signal was later subtracted from these spectra. The V_2O_5/ZrO_2 and ZrO_2 catalysts were not run in the series of experiments described above, but data is available from previous experiments using methanol (semiconductor grade, Fisher Scientific) introduced at about 1.15% concentration by bubbling the gas through a methanol bubbler (held at $-20\,^{\circ}C$ in a recirculating bath of water and ethylene glycol). The $CH_3OH/O_2/He$ flow (1/15/84 molar ratio to ensure oxidizing conditions) was held at 100 ml/min in these experiments. For pure zirconia, spectra in the C–H stretching region were obtained from vacuum dosing experiments using the traditional cell (saturation of ZrO_2 under 10 Torr methanol, followed by evacuation and spectral acquisition).

2.2.3. In situ UV-Vis DRS spectroscopy

The UV-Vis DRS spectra were recorded on a Varian Cary 5E UV-Vis-NIR spectrophotometer operated in diffuse reflectance mode (DRS). Unlike transmission UV-Vis, which follows Beer's Law, the Kubelka–Munk signal intensity function (KM) is used in DRS to linearize the

diffuse reflectance signal against chromophore concentration [36,37]. However, despite the advantage in signal-to-noise relative to transmission mode at low concentrations, the KM function generally fails at higher concentrations and yields spectra with unacceptable SN ratios. Therefore, all samples in the current study are limited to 5% V_2O_5 or lower loading. The *in situ* experiments were performed in the Praying Mantis Diffuse Reflectance Attachment manufactured by Harrick Scientific Co. The samples studied with UV-Vis DRS (1% V_2O_5/SiO_2, 4% V_2O_5/ZrO_2, and 5% V_2O_5/Al_2O_3) were all pretreated at 450 °C for 1 h in flowing O_2/He (same ratio as before, 100 ml/min). *In situ* experiments were performed using methanol introduced from an ice-bath bubbler with a CH_3OH/O_2/He ratio of 4/13/83 and a flowrate of 100 ml/min. All spectra were recorded at 230 °C for the UV-Vis DRS experiments.

3. Results

3.1. In situ Raman spectra

Raman spectra are presented in figures 1–4 for supported vanadium oxide catalysts (vanadia supported on Al_2O_3, TiO_2, SiO_2, Nb_2O_5, and ZrO_2) under fully oxidizing conditions and in a reaction stream of CH_3OH/O_2/He gases at different temperatures. Two regions of the Raman spectra were monitored: the 100–1200 cm^{-1} metal–oxygen vibrational region and the 2800–3000 cm^{-1} methoxy C–H stretching vibrational region. In the metal–oxygen vibrational region, the Raman spectra were collected from 600 to 1100 cm^{-1} (SiO_2- and $A1_2O_3$-supported samples, figure 2), or from 700 to 1100 cm^{-1} (TiO_2- and ZrO_2-supported samples, figures 1 and 3(A), respectively), or from 800 to 1100 cm^{-1} (Nb_2O_5-supported samples, figure 3(B)). Raman spectra in the methoxy region are given for the vanadia/titania and vanadia/silica systems in figure 4. The lower wavenumber regions for all the supported vanadia samples did not provide any additional information and the pure oxide supports exhibited no changes in the metal–oxygen region upon introduction of methanol into the gas stream.

In the metal–oxygen stretching region, figures 1–3 show the *in situ* Raman spectra at different temperatures (230, 300, and 360 °C) in the presence of: (i) O_2 ((a), (c), and (e)), or (ii) CH_3OH/O_2/He ((b), (d), and (f)) gas streams. Under fully oxidized conditions, these Raman spectra exhibit bands at ∼1030 and ∼920–950 cm^{-1} that are characteristic of the supported vanadia surface species. The Raman band at ∼1030 cm^{-1}, assigned to the symmetric stretch of a mono-oxo terminal V=O bond [1,3,20,21,30], is relatively sharp and intense. The much broader and weaker band at ∼920–950 cm^{-1} is assigned to the bridging V–O–V stretching modes, and is absent in the case of monomeric 3% V_2O_5/SiO_2. Figure 1 also shows that the V=O band shifts slightly to higher wavenumbers, from 1028 to 1032 cm^{-1}, with increased vanadia loading in

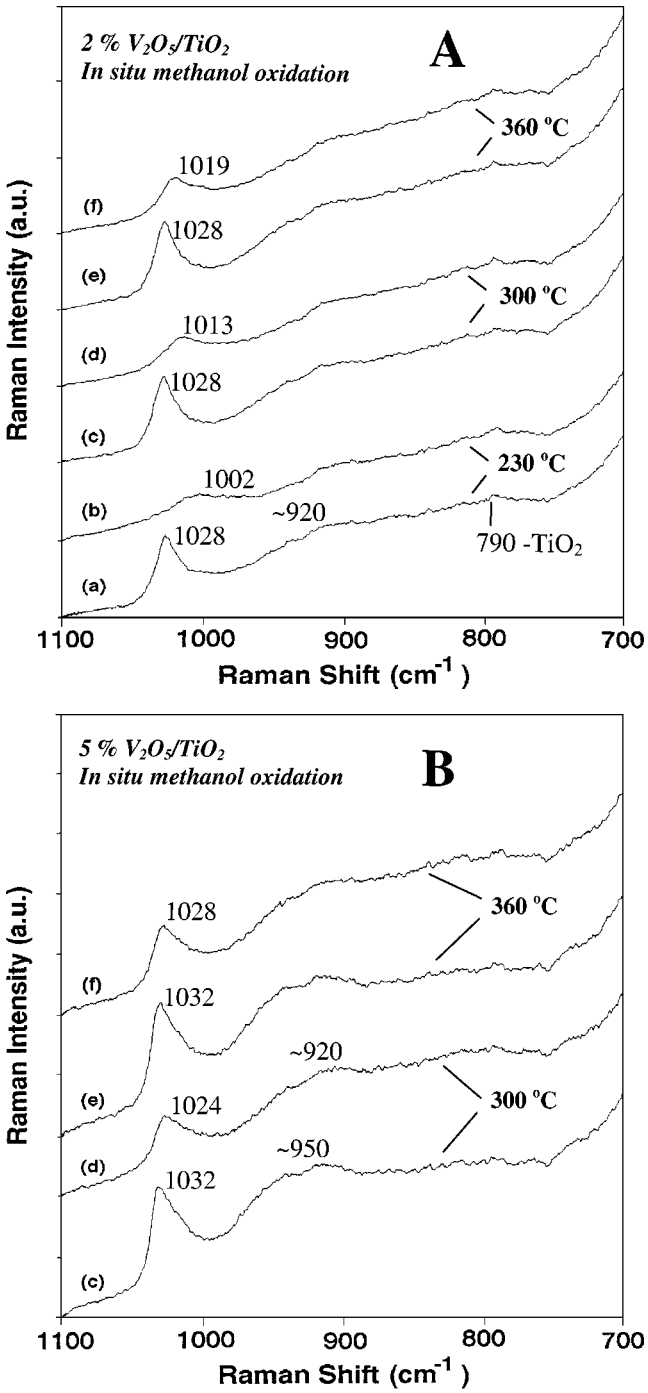

Figure 1. *In situ* Raman spectra in the metal–oxygen stretching region of (A) 2% V_2O_5/TiO_2 catalysts and (B) 5% V_2O_5/TiO_2 catalysts under the following gas flows: (a) O_2 at 230 °C, (b) CH_3OH/O_2/He at 230 °C, (c) O_2 at 300 °C, (d) CH_3OH/O_2/He at 300 °C, (e) O_2 at 360 °C, and (f) CH_3OH/O_2/He at 360 °C.

V_2O_5/TiO_2. A similar shift and an increase in relative intensity are also observed for the bridging V–O–V polymerized mode in V_2O_5/TiO_2. However, in contrast to these relatively intense V=O and V–O–V Raman bands, the inability to directly detect bridging V–O–support vibrations in all cases suggests that the V–O–support modes have very weak Raman scattering cross-sections.

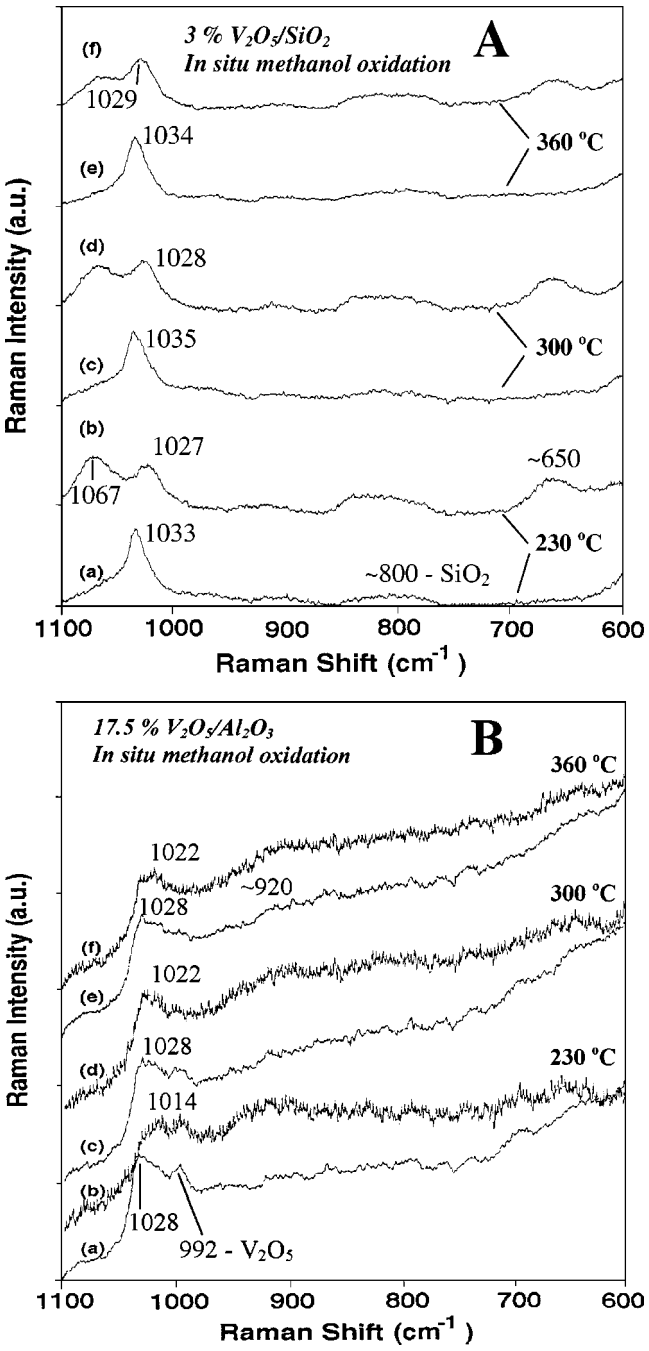

Figure 2. *In situ* Raman spectra in the metal–oxygen stretching region of (A) 3% V_2O_5/SiO_2 catalysts and (B) 17.5% V_2O_5/Al_2O_3 catalysts under the following gas flows: (a) O_2 at 230 °C, (b) CH_3OH/O_2/He at 230 °C, (c) O_2 at 300 °C, (d) CH_3OH/O_2/He at 300 °C, (e) O_2 at 360 °C, and (f) CH_3OH/O_2/He at 360 °C.

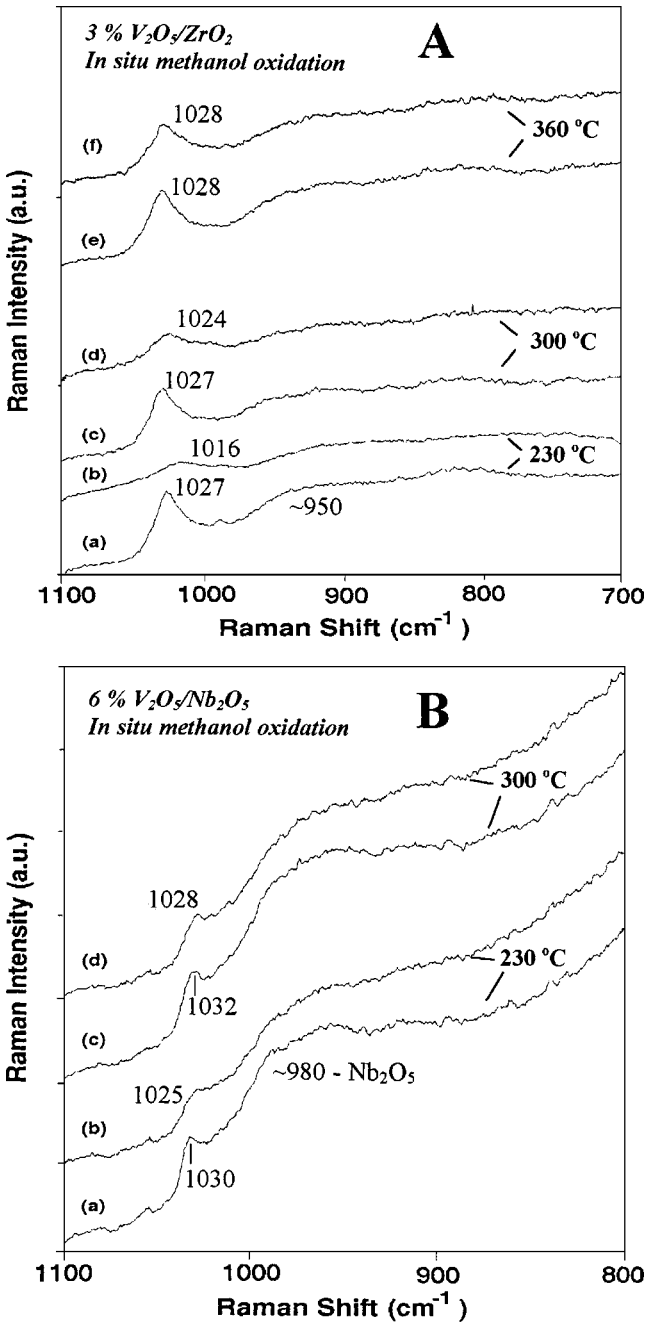

Figure 3. *In situ* Raman spectra in the metal–oxygen stretching region of (A) 3% V_2O_5/ZrO_2 catalysts and (B) 6% V_2O_5/Nb_2O_5 catalysts under the following gas flows: (a) O_2 at 230 °C, (b) CH_3OH/O_2/He at 230 °C, (c) O_2 at 300 °C, (d) CH_3OH/O_2/He at 300 °C, (e) O_2 at 360 °C, and (f) CH_3OH/O_2/He at 360 °C.

Upon introduction of methanol into the O_2/He gas stream, both the terminal V=O and bridging V–O–V bands decrease in intensity and shift to lower wavenumbers for all the supported vanadia catalysts. The decrease in intensity and downward shift of these Raman bands is more pronounced for the lower reaction temperature (230 °C) than for the higher reaction temperatures (300 and 360 °C). For example, on 2% V_2O_5/TiO_2 (figure 1(A)) the V=O band at 1028 cm^{-1} shifts to 1002 cm^{-1} at 230 °C, to 1013 cm^{-1} at 300 °C, and to 1019 cm^{-1} at 360 °C. At higher vanadia loading the downshift in the V=O band seems to be somewhat less, since the V=O band at 1032 cm^{-1} in 5% V_2O_5/TiO_2 (figure 1(B)) shifts to 1024 cm^{-1} at 300 °C, and to 1028 cm^{-1} at 360 °C. The V–O–V band at ~950 cm^{-1} in this catalyst is also clearly seen to decrease in intensity during methanol oxidation, and the maximum of this broad feature appears to shift down toward ~920 cm^{-1}. Similar downshifts in the V=O and V–O–V bands were also ob-

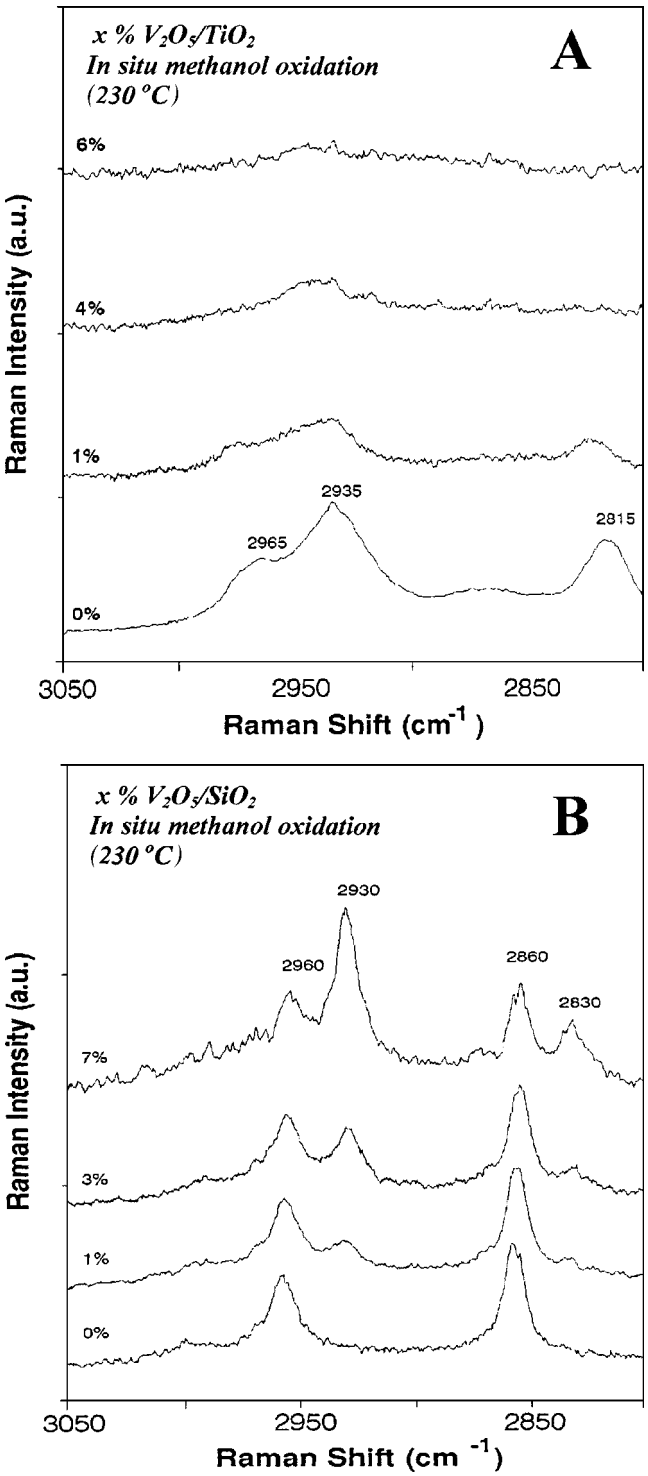

Figure 4. *In situ* Raman spectra in the C–H stretching region of (A) V_2O_5/TiO_2 catalysts and (B) V_2O_5/SiO_2 catalysts under CH_3OH/O_2/He flow at 230 °C.

served for the other supported vanadia catalysts (figures 2 and 3). For example, at 230 °C the V=O band shifts from 1033 to 1027 cm^{-1} for 3% V_2O_5/SiO_2 (figure 2(A); assignments for the Raman bands at 1067 and 650 cm^{-1} are given below), from 1028 to 1014 cm^{-1} for 17.5% V_2O_5/Al_2O_3 (figure 2(B); noise in methanol oxidation spectra is due to the onset of fluorescence in these samples), from 1027 to 1016 cm^{-1} for 3% V_2O_5/ZrO_2 (figure 3(A)), and from 1030 to 1025 cm^{-1} for 6% V_2O_5/Nb_2O_5 (figure 3(B)).

The surface methoxy (–OCH_3) C–H stretching region at 2800–3000 cm^{-1} was also monitored by *in situ* Raman spectroscopy for the V_2O_5/TiO_2 and V_2O_5/SiO_2 catalysts during the flow of the CH_3OH/O_2/He gas mixture at 230 °C (figure 4). On the pure TiO_2 support, Ti–OCH_3 bands occur at 2815, 2935, and 2965 cm^{-1} (figure 4(A)). The first two bands are assigned to intense Fermi resonances between the symmetric methyl stretch, $\nu_s(CH_3)$ at 2935 cm^{-1}, and first overtone of the symmetric methyl bending mode, $2\delta_s(CH_3)$ at 2815 cm^{-1}, whereas the 2965 cm^{-1} band is assigned to the asymmetric methyl stretching mode, $\nu_{as}(CH_3)$ [32,38]. These bands progressively decrease with increasing surface vanadia coverage and essentially disappear at near monolayer loadings (5 wt% V_2O_5), indicating that no V–OCH_3 species are detected in the V_2O_5/TiO_2 systems by Raman spectroscopy. The pure SiO_2 support shows bands at 2960 and 2860 cm^{-1} during methanol oxidation conditions (figure 4(B)), assigned to the $\nu_s(CH_3)$ and $2\delta_s(CH_3)$ modes of Si–OCH_3 species, respectively [30]. Unlike V_2O_5/TiO_2, however, increasing the vanadia loading from 1 to 7% V_2O_5/SiO_2 creates new Raman bands at 2830 and 2930 cm^{-1} due to the presence of V–OCH_3 species (assignments analogous to Ti–OCH_3 and Si–OCH_3, with the exact frequencies depending on the specific metal cation). Lower frequency bands at 1067 and 650 cm^{-1} in the V_2O_5/SiO_2 catalysts are also indicative of adsorbed methoxy species (figure 2(A)). The band at 1067 cm^{-1} is assigned to a C–O methoxy stretching mode [30,32,38], while the band at 650 cm^{-1} has been assigned to a V–O stretch in the V–OCH_3 complex [30].

The methoxy Raman vibrations for vanadia/zirconia catalysts (spectra in methoxy region not shown for brevity) were found to behave similarly to those of the vanadia/titania catalysts, while the methoxy vibrations on vanadia/alumina catalysts were obscured by fluorescence in this spectral region. Raman spectra were not collected in the methoxy region for the vanadia/ceria or vanadia/niobia catalysts.

3.2. In situ IR spectra

The IR spectra of the supported vanadia catalysts (vanadia supported on Al_2O_3, TiO_2, SiO_2, CeO_2, and ZrO_2) are presented in figures 5–10. In contrast to the relatively low Raman activity of the oxide supports, the IR absorbance of these supports is quite high in the metal–oxygen region and limits the amount of useful spectral information that can be obtained from the corresponding supported vanadia catalysts. For example, figures 5 and 6 show that the transmission cutoff (infinite absorbance) of thin catalyst wafers occurs below 900 cm^{-1} for 5% V_2O_5/TiO_2, below 950 cm^{-1} for 20% V_2O_5/Al_2O_3, and below 700 cm^{-1} for 3% V_2O_5/CeO_2. For the vanadia/silica and vanadia/zirconia catalysts this cutoff occurs below

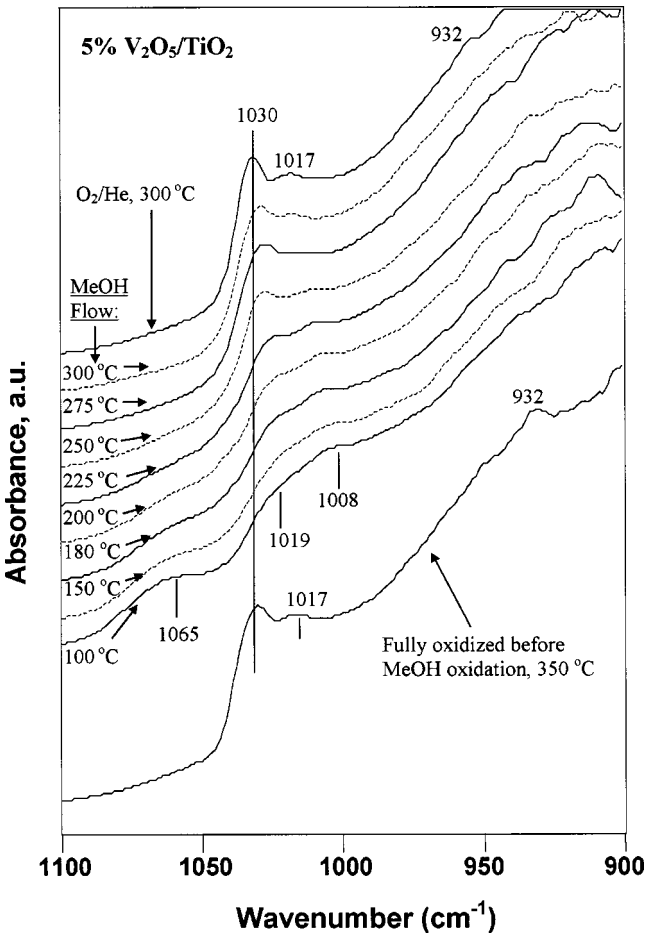

Figure 5. *In situ* IR spectra in the metal–oxygen stretching region of the 5% V_2O_5/TiO_2 catalyst under O_2/He and CH_3OH/O_2/He gas flows at various temperatures.

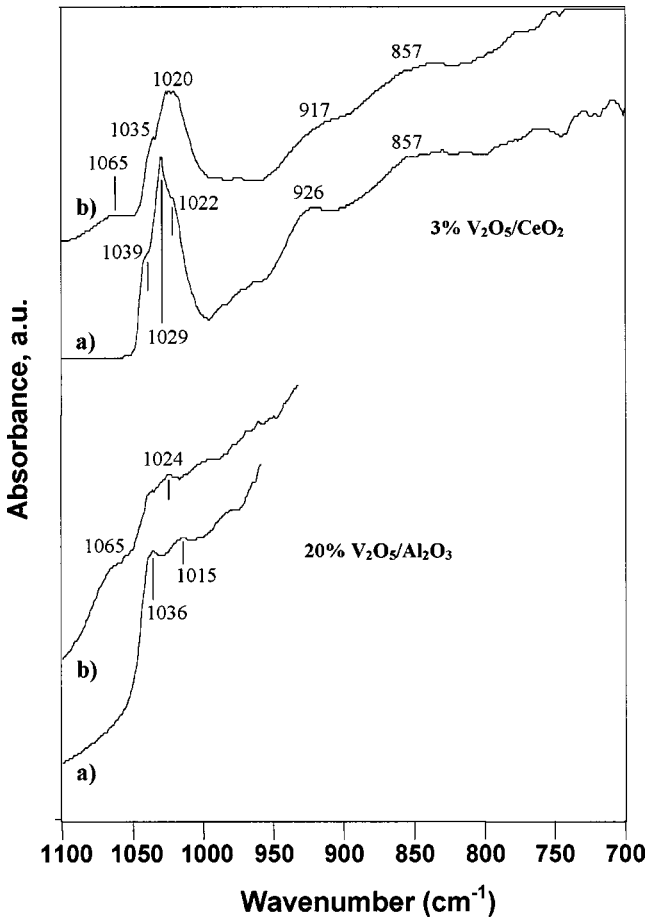

Figure 6. *In situ* IR spectra in the metal–oxygen stretching region of the 3% V_2O_5/CeO_2 and 20% V_2O_5/Al_2O_3 catalysts under the following gas flows: (a) O_2/He at 350 °C and (b) CH_3OH/O_2/He at 230 °C.

$\sim$1050 cm^{-1} (for the wafer thicknesses used in the present study), which completely obscures the vanadium–oxygen vibrations in this region for these catalysts. However, for the more transparent catalysts (vanadia supported on TiO_2, Al_2O_3, and CeO_2) the vanadium–oxygen vibrational modes in the 900–1100 cm^{-1} region can be detected. Moreover, interpretation of bands from surface vanadia species on these supports is simplified because the IR spectra (not shown) of the pure TiO_2, Al_2O_3, and CeO_2 supports remain essentially featureless above their cutoff until $\sim$1100 cm^{-1}.

Figures 5 and 6 show that the terminal V=O IR bands are clearly resolved in the fully oxidized samples of vanadia supported on TiO_2 and Al_2O_3 with the same, coincident frequencies at $\sim$1030 cm^{-1} as were observed for the V=O stretching modes in the Raman spectra (figures 1–3). The Raman frequency of the V=O band in 3% V_2O_5/CeO_2, measured elsewhere to be 1028 cm^{-1} [20], is also essentially coincident with the IR band at 1029 cm^{-1} in figure 6. Additional shoulders appear on these bands at 1017 cm^{-1} for 5% V_2O_5/TiO_2 (figure 5), at 1039 and 1022 cm^{-1} for 3% V_2O_5/CeO_2 (figure 6), and at 1015 cm^{-1} for 20% V_2O_5/Al_2O_3 (figure 6). These shoulders are most likely due to the terminal V=O bonds in polymerized surface vanadia species (see section 4) and suggest that somewhat better spectral resolution is achieved with IR than with Raman in this wavenumber region. The bridging V–O–V mode of these polymerized surface vanadia species is observed as a broad band at $\sim$926 cm^{-1} in 3% V_2O_5/CeO_2 and at $\sim$932 cm^{-1} in 5% V_2O_5/TiO_2, and is again very similar to the corresponding Raman band position. Finally, another weak IR band in this region for 3% V_2O_5/CeO_2 at $\sim$857 cm^{-1} may be the asymmetric VO_x stretching modes, since CeO_2 has no band in this region.

The infrared spectra also provide additional information about the surface vanadia species in the V=O overtone region (1900–2100 cm^{-1}), as is shown in figure 7. For the fully oxidized catalysts, all samples have a single V=O overtone that is relatively weak and broad with a maximum at 2036 cm^{-1}. This frequency is slightly less than twice the fundamental frequency (2×1030 $cm^{-1} = 2060$ cm^{-1}) and indicates some anharmonicity in the V=O vibrator [39,40]. Interestingly, the V=O overtone in the 3% V_2O_5/ZrO_2 sample is clearly detectable, despite an inability to resolve the fundamental, because the IR absorbance of the ZrO_2 support is very low in the overtone region. Unfortunately, silica has strong IR absorbance in both the overtone and

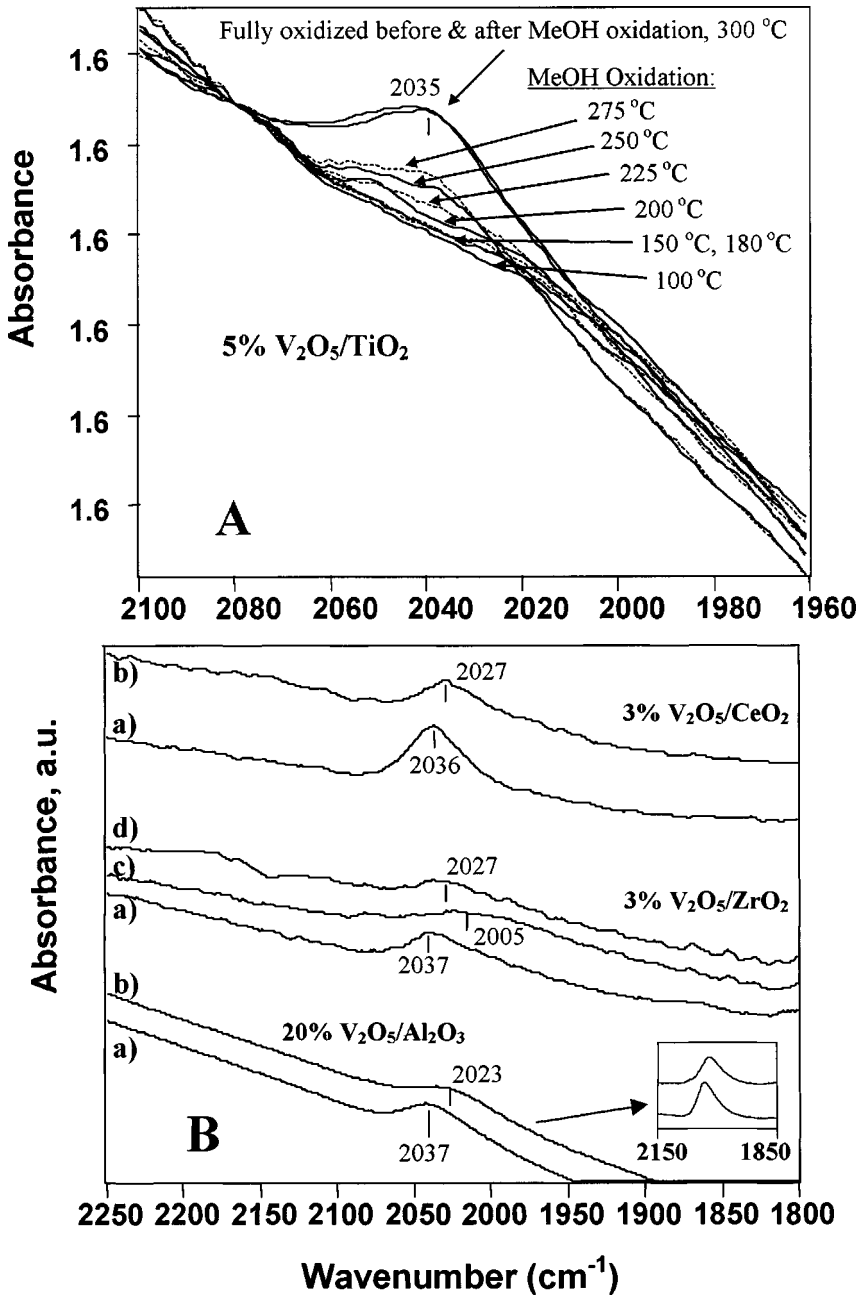

Figure 7. *In situ* IR spectra in the metal–oxygen overtone region of (A) the 5% V_2O_5/TiO_2 catalyst under O_2/He and CH_3OH/O_2/He gas flows at various temperatures and (B) the 3% V_2O_5/CeO_2, 3% V_2O_5/ZrO_2, and 20% V_2O_5/Al_2O_3 catalysts under the following gas flows: (a) O_2/He at 350 °C, (b) 2000 ppm CH_3OH/O_2/He at 230 °C, (c) 1% CH_3OH/O_2/He at 230 °C, and (d) 1% CH_3OH/O_2/He at 300 °C. The insert shows the baseline corrected spectra of the V=O overtones in 20% V_2O_5/Al_2O_3.

fundamental regions and prohibits any IR detection of V=O modes in 3% V_2O_5/SiO_2.

During methanol oxidation, the *in situ* IR spectra shown in figures 5–7 indicate the same decreases in the terminal V=O and bridging V–O–V band intensities as were observed in the *in situ* Raman spectra for the supported vanadia catalysts. The downward shift in the terminal V=O bond is also observed to follow the same trend as in the Raman spectra. Specifically, figure 5 shows that 5% V_2O_5/TiO_2 exhibits a downshift in the V=O band from 1030 to 1019 cm^{-1} for a temperature of 100 °C under methanol oxidation. The original band frequency is gradually recovered as the temperature is raised to 300 °C under methanol flow. The shoulder at 1017 cm^{-1} also shifts down to 1008 cm^{-1} at 100 °C under methanol oxidation and is recovered by 300 °C. At 230 °C, the terminal V=O band in 3% V_2O_5/CeO_2 shifts from 1029 to 1020 cm^{-1} with a reduction in intensity, while in the 20% V_2O_5/Al_2O_3 catalyst this band shifts from 1036 to 1024 cm^{-1} (see figure 6). Figure 7 shows similar behavior in the V=O overtones, with shifts from the original ~2036 cm^{-1} band position under fully oxidized conditions to 2023–2027 cm^{-1} un-

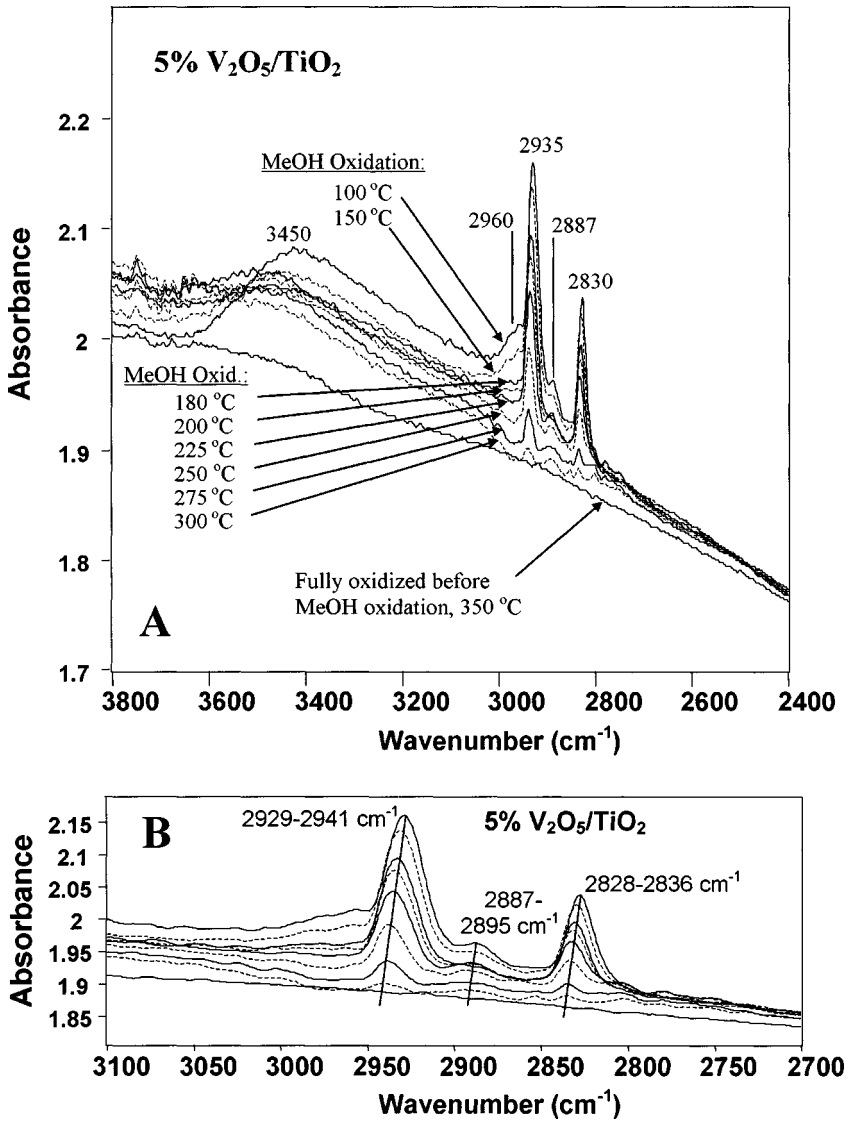

Figure 8. *In situ* IR spectra in the C–H stretching region of the 5% V_2O_5/TiO_2 catalyst under O_2/He and CH_3OH/O_2/He gas flows at various temperatures. Temperatures and conditions in the rescaled figure (B) are the same as in (A).

der methanol oxidation at 230–300 °C. While all catalysts showed a reduction in the V=O overtone band intensity during methanol oxidation, the 5% V_2O_5/TiO_2 sample appears to be most severely affected because the overtone band is nearly eliminated at lower temperatures. During methanol oxidation at 230 °C, the V–O–V mode is seen to shift from 926 to 917 cm^{-1} in 3% V_2O_5/CeO_2 with a reduction in intensity and the band at 857 cm^{-1} in this catalyst, as well as the V–O–V band at 932 cm^{-1} in 5% V_2O_5/TiO_2, exhibit a reduction in intensity (see figures 5 and 6).

The *in situ* IR spectra of adsorbed methoxy intermediate species are given in figures 8–10. The most striking observation is that the methoxy C–H stretching IR bands are observed on all catalysts and supports tested, in contrast to the corresponding Raman spectra. As in the Raman spectra, the methoxy vibrations in this region consist of two bands in Fermi resonance at 2920–2960 and 2815–2860 cm^{-1} assigned to the $\nu_s(CH_3)$ and $2\delta_s(CH_3)$ modes, respectively. A weaker shoulder at 2960–2990 cm^{-1} is assigned to $\nu_{as}(CH_3)$. A weak band not seen in Raman also appears at 2880–2905 cm^{-1} and is assigned to overlapping modes from a second methoxy overtone band, $2\delta_{as}(CH_3)$ at ~2905 cm^{-1}, and the symmetric C–H stretch of surface formate (HCOO–) species, ν_s(C–H) at ~2880 cm^{-1}, formed by readsorption of the formaldehyde product during *in situ* methanol oxidation [32,38]. More importantly, V–OCH_3 species are indicated on all the supported vanadia systems by the presence of bands at ~2932 and at ~2832 cm^{-1} that are of different frequency than the oxide support methoxy bands (see figures 9 and 10). On pure ceria and alumina supports there appear to be two surface methoxy species based on the presence of four bands in the C–H stretching region, but these frequencies remain distinct from those of V–OCH_3. Moreover, the surface vanadia monolayers on TiO_2, CeO_2, ZrO_2, and Al_2O_3 exhibit only V–OCH_3 bands and appear to have no access to exposed support cation

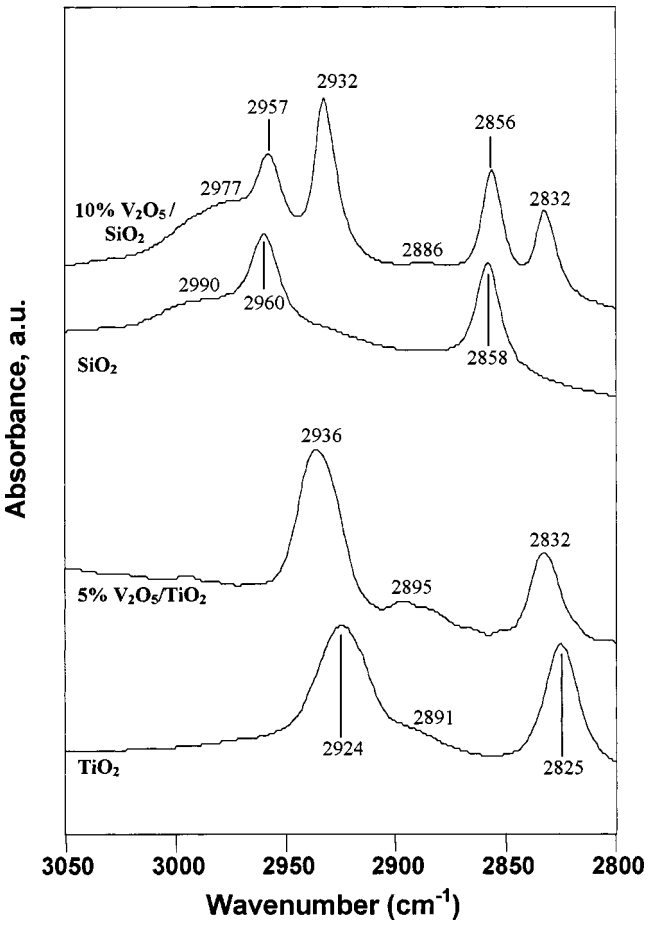

Figure 9. *In situ* IR spectra in the C–H stretching region of 10% V_2O_5/SiO_2, SiO_2, 5% V_2O_5/TiO_2, and TiO_2 catalysts under CH_3OH/O_2/He gas flow at 230 °C.

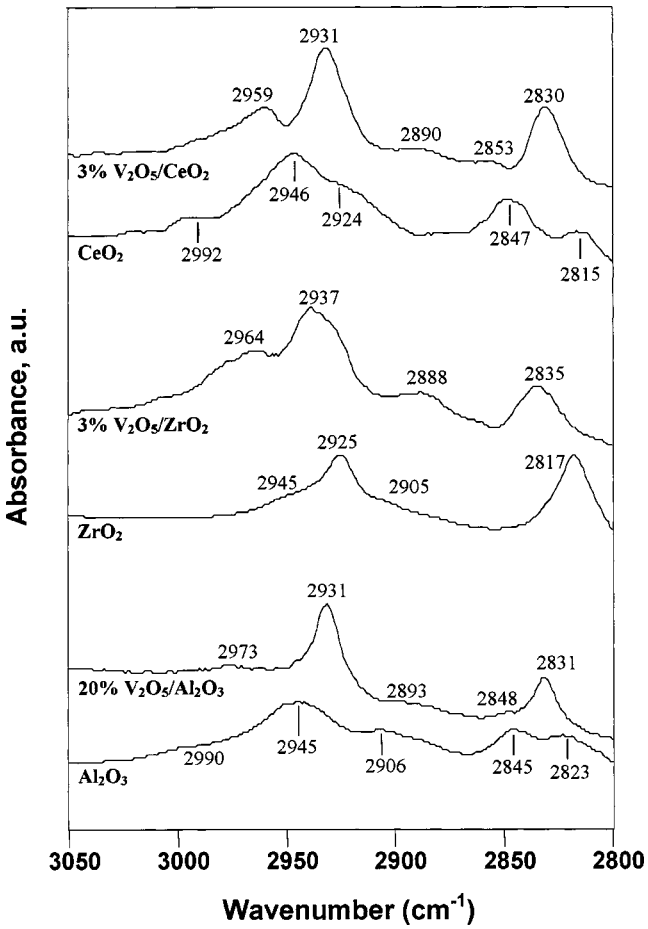

Figure 10. *In situ* IR spectra in the C–H stretching region of 3% V_2O_5/CeO_2, CeO_2, 3% V_2O_5/ZrO_2, ZrO_2, 20% V_2O_5/Al_2O_3, and Al_2O_3 catalysts under the CH_3OH/O_2/He gas flow at 230 °C.

sites for the formation of support methoxy species. In contrast, the 10% V_2O_5/SiO_2 catalyst contains both V–OCH_3 and Si–OCH_3 bands in the IR spectrum due to the presence of exposed silica surface sites.

The presence of adsorbed methoxy species during methanol oxidation is also indicated in the metal–oxygen stretching region (figures 5 and 6) by a C–O stretching mode at 1065 cm^{-1} on the TiO_2-, CeO_2-, and Al_2O_3-supported vanadia catalysts. In the Raman spectra, this mode was only observed on the vanadia/silica system, which is dominated by Si–O modes in IR and cannot be compared. Other low frequency –OCH_3 modes (not shown) include the symmetric and asymmetric methyl bends at ~1430 and ~1455 cm^{-1}, respectively, and a C–O rocking mode at ~1150 cm^{-1}. Also, a weak OH deformation mode at ~1370 cm^{-1} is usually observed due to the presence of an intact, but strongly adsorbed, Lewis-bound methanol species that coexists on supported vanadia catalysts as a minority species along with the more abundant, dissociatively adsorbed methoxy species [32,38]. The relative intensity of the surface methoxy C–H stretching bands is usually much stronger than that of the corresponding C–H deformation modes on the ionic oxide supports, where the deformation modes are hardly visible. Formaldehyde readsorption in thicker, mass-transfer limited wafers can also create strong formate bands in this region (also not shown) that occur at 1550 cm^{-1} (O–C–O asymmetric stretch) and 1360/1380 cm^{-1} (O–C–O symmetric stretches) [12,32,35,38].

The intensity of the adsorbed methoxy species decreases as the temperature is increased under steady-state methanol oxidation (see figure 5(A) for 5% V_2O_5/TiO_2). For transmission IR experiments, Beer's Law dictates that these intensities are proportional to the surface methoxy concentration. The decrease in surface methoxy concentration is also accompanied by an upward shift in the methoxy IR band positions, as shown in figure 5(B). The primary V–OCH_3 bands are seen to shift from 2929 and 2828 cm^{-1} at low temperatures and high methoxy coverage to 2941 and 2836 cm^{-1} at high temperatures and low methoxy coverage, an effect that is most likely due to increased lateral interactions (hydrogen-bonding, etc.). Transient experiments (not shown) also demonstrated that removal of methanol from the vapor phase resulted in immediate loss of adsorbed methoxy signals for the vanadia monolayers on titania, ceria, zirconia, and alumina at temperatures above 200 °C (vanadia/silica not tested). The surface methoxy species were far more stable on the pure oxide supports at all tem-

peratures and on the supported vanadia systems at 100 °C. Finally, the band at ~3450 cm^{-1} in figure 5(A) is assigned to a hydroxyl OH group that is hydrogen-bonded to the adsorbed methoxy intermediates and exhibits the same decrease in concentration with increased temperature as the methoxy species.

3.3. In situ UV-Vis DRS spectra

The UV-Vis DRS spectra of the supported vanadia catalysts (vanadia supported on Al_2O_3, SiO_2, and ZrO_2) at 230 °C are presented in figure 11. The intense, broad bands located above 25,000 cm^{-1} are assigned to ligand–metal charge transfer (LMCT) transitions involving primarily the charge transfer from oxygen ligands to V^{5+} metal cations [36,37]. In the fully oxidized state, this band is most intense for vanadia on silica, slightly less intense for vanadia on alumina, and was significantly less intense for vanadia on zirconia. Introduction of methanol into the O_2/He stream results in a decrease in the intensity of these bands, as well as a shift in the band maxima to higher wavenumbers. For example, the band maximum of 4% V_2O_5/ZrO_2 shifts from ~33,000 to ~38,000 cm^{-1} upon introduction of methanol, while that of 1% V_2O_5/SiO_2 shifts from ~38,000 to ~41,000 cm^{-1}. The 5% V_2O_5/Al_2O_3 catalyst was least sensitive to the decrease in band intensity and shifts, changing only slightly during methanol flow. Interestingly, complete reduction of the V^{5+} with hydrogen does not fully diminish the LMCT band in these catalysts (40–90% of band area is retained depending on the catalyst) [41], indicating that LMCT transitions also occur for the reduced V^{3+}/V^{4+} metal cations in this region, as well.

The d–d transitions of the V^{3+}/V^{4+} reduced vanadia cations occur as very weak and broad bands in the visible region (10,000–30,000 cm^{-1}) [36,37]. These are indicated in the insert of figure 11 (note ordinate scale), where it can be seen that an increase in surface V^{3+}/V^{4+} species occurs during methanol oxidation over the vandia/alumina and vanadia/zirconia catalysts. The 1% V_2O_5/SiO_2 catalyst did not produce a signal increase in this region and apparently remains fully oxidized in the flow of CH_3OH/O_2/He (gas stream molar ratio of 4/13/83). Unfortunately, the broad and weak nature of these d–d transition bands prevents quantification of these species or identification of the individual surface V^{3+} and V^{4+} components.

These qualitative observations are also consistent with the edge energy calculations given in table 1, in which the band edge energies (E_g) of the V^{5+} LMCT transition (>25,000 cm^{-1}) have been determined by finding the x-intercept of the low energy linear rise in $[F(R_\infty) \times h\nu]^2$ vs. $h\nu$, where $F(R_\infty)$ is the Kubelka–Munk DRS intensity and $h\nu$ is the energy of the incident photon [30]. All three catalysts exhibit comparable edge energies in the fully oxidized state, although the slightly lower E_g of 4% V_2O_5/ZrO_2 may be due to the presence of additional V–O–V functionalities on this monolayer sample that do not occur in the sub-monolayer 1% V_2O_5/SiO_2 and 5% V_2O_5/Al_2O_3 samples. However, the vanadia/silica sample exhibits a large decrease in edge energy upon introduction of methanol into the gas flow, and does not exhibit an increase in the V^{3+}/V^{4+} d–d transition region at 10,000–

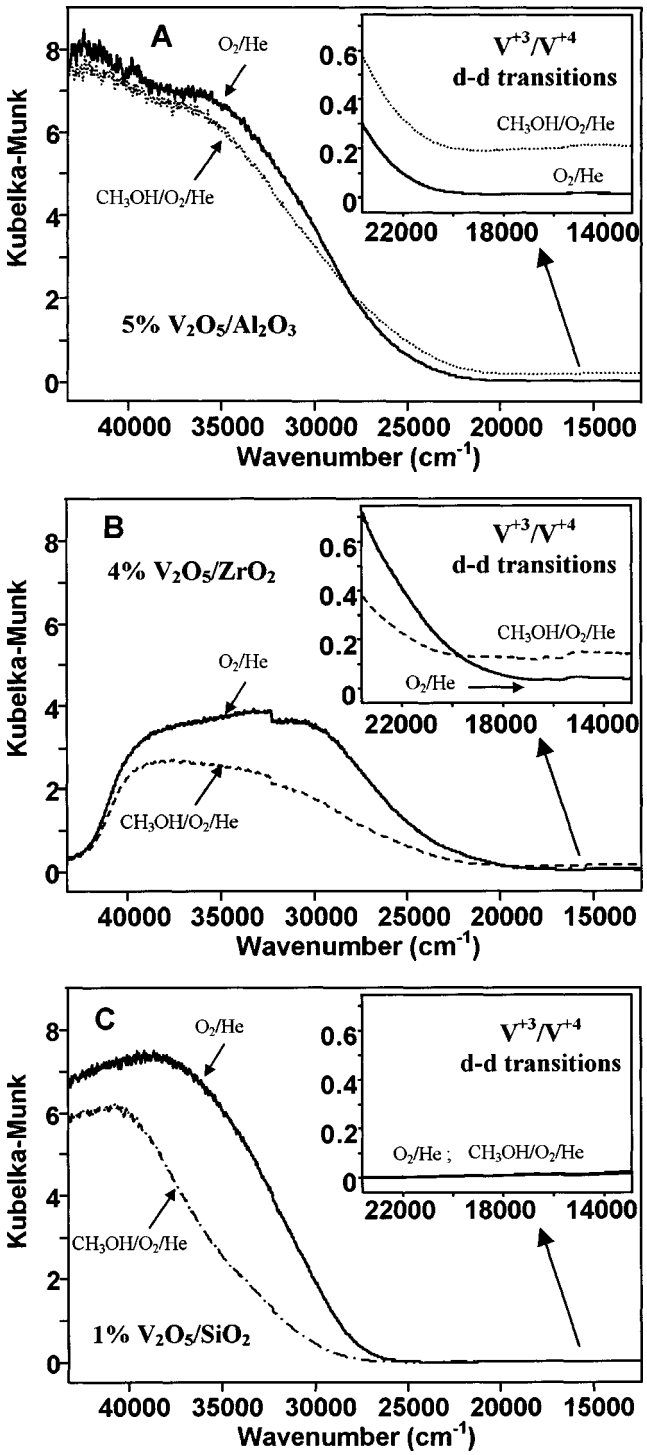

Figure 11. *In situ* UV-Vis DRS spectra at 230 °C for supported vanadia catalysts under gas flows of O_2/He and CH_3OH/O_2/He: (A) 5% V_2O_5/Al_2O_3, (B) 4% V_2O_5/ZrO_2, and (C) 1% V_2O_5/SiO_2. The insert shows an expanded view of the d–d transition region. Note that the slight discontinuity in (B) (4% V_2O_5/ZrO_2 spectra) is due to the sensitivity of this sample to an instrumental lamp change at the wavenumber of the discontinuity (~32,000 cm^{-1}).

Table 1
UV-Vis DRS edge energies (V^{5+} LMCT band) during methanol oxidation at 230 °C.

Catalyst	E_g (eV)		ΔE_g (eV)[a]
	O_2/He at 230 °C	CH_3OH/O_2/He at 230 °C	CH_3OH/O_2/He at 230 °C
1% V_2O_5/SiO_2	3.74	4.31	0.57
5% V_2O_5/Al_2O_3	3.61	3.65	0.04
4% V_2O_5/ZrO_2	3.14	3.29	0.15

[a] $\Delta E_g = E_g(\text{rxn}) - E_g(O_2/\text{He})$.

30,000 cm^{-1}. By contrast, relatively small changes in the V^{5+} LMCT band intensity and E_g are seen to occur for vanadia/alumina and vanadia/zirconia, despite the partial reduction of surface V^{5+} indicated by the presence of d–d transitions at 10,000–30,000 cm^{-1} from reduced surface V^{3+}/V^{4+} species. Therefore, the surface vanadia LMCT band does not appear to correlate exclusively with the extent of surface V^{5+} reduction during methanol oxidation.

4. Discussion

4.1. Molecular structures of dehydrated, fully oxidized VO_4 surface species

The dehydrated Raman, IR, and UV-Vis DRS spectra of supported vanadia catalysts reported in the present study are consistent with the molecular structural models proposed from previous characterization studies [1–4,12–23,23–32]. The UV-Vis DRS spectra indicate that the surface vanadia species is in the fully oxidized V^{5+} state under O_2/He flow based on the intense V^{5+} LMCT band above 25,000 cm^{-1} for surface vanadia on alumina, zirconia, and silica. There are also no d–d transition bands from reduced surface V^{3+}/V^{4+} species in the visible region (10,000–30,000 cm^{-1}) for these catalysts under oxidizing conditions. In the dehydrated Raman spectra, there are two main bands at 1016–1040 and 840–940 cm^{-1} that are assigned to a terminal V=O bond and bridging V–O–V functionalities, respectively. The bridging V–O–V Raman band increases substantially in intensity relative to the V=O band as the surface vanadia coverage is increased. Therefore, two surface vanadium oxide species are present on the oxide supports: an isolated tetrahedral vanadium oxide species possessing a single, mono-oxo V=O terminal bond and three V–O–support bonds (see below for discussion of mono-oxo structure), and a polymeric vanadium oxide species possessing both V=O and V–O–V functionalities. The ratio of polymerized to monomeric surface vanadia species increases with loading, except that in V_2O_5/SiO_2 only monomeric species are detected (i.e., no band at ~920 cm^{-1} even at high loading [30]). A schematic drawing of these fully oxidized molecular structures is given in figure 12.

The appearance of the same V=O and V–O–V bands at nearly identical frequencies in the IR spectra of supported vanadia catalysts further supports the proposed molecular

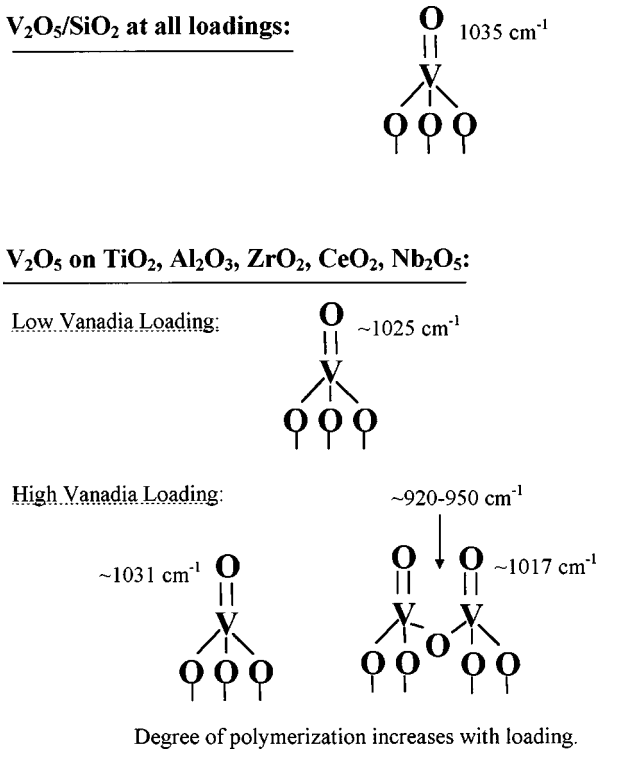

Figure 12. Schematic diagram of the molecular structures of fully oxidized supported vanadia surface species.

structure. In addition, the coincidence of Raman and IR frequencies at ~1030 cm^{-1} for the terminal vanadium–oxygen bond is strong evidence for the presence of a mono-oxo, V=O terminal double bond. A di-oxo, O=V=O species would be expected to have both symmetric and asymmetric stretching modes separated by about 20–30 cm^{-1} and having opposite relative intensities in Raman and IR (the symmetric stretch most likely having the greatest Raman intensity) [11,27,42]. The shoulders present in the IR spectra at 1039 and 1022 cm^{-1} in 3% V_2O_5/CeO_2 and at ~1017 cm^{-1} in 5% V_2O_5/TiO_2 and 20% V_2O_5/Al_2O_3 are most likely due to mono-oxo, V=O terminal double bonds within VO_4 units of slightly different local symmetries (i.e., polymerized surface vanadia species). If the IR shoulders were the asymmetric stretches of a di-oxo species then their band positions would have dominated the Raman spectra. Instead, the V=O band maxima in both IR and Raman occur at the same frequency of ~1030 cm^{-1}. The IR overtones similarly indicate the presence of a mono-oxo V=O terminal double bond, since only a single band at ~2035 cm^{-1} is detected at nearly twice the frequency of the fundamental vibration. A di-oxo species would have produced three bands in this region due to the combination band and two overtones of the symmetric and asymmetric O=V=O stretches [27].

The terminal V=O double bond at ~1030 cm^{-1} is rather insensitive to the specific oxide support and shifts upward only about ~5 cm^{-1} from low surface vanadia coverages to high coverages (corresponding to a slight shortening of bond length). This insensitivity is most likely due to the

concentration of vibrational potential energy in the terminal V=O bonds, which effectively isolates the mono-oxo vanadyl species as a diatomic vibrator. In fact, such a diatomic approximation has also been used successfully to correlate the Raman V=O frequencies in bulk and supported metal oxides to the V=O bond strengths and bond lengths [1,28]. However, the slight shift in V=O band position with increased surface vanadia coverage and similar (± 5 cm^{-1}) variation in band position with changes in the specific oxide support indicate some weak vibrational influence from the surrounding environment. The first anharmonicity constant for such a diatomic vibrator is a measure of oscillatory dampening that is sensitive to external vibrational perturbations, and is calculated from the V=O fundamental (ν^0) and first overtone (ν^1) as $(2\nu^0 - \nu^1)/2$ [40] to be about 12.5 cm^{-1} using the present results. For a free, gas-phase V–O diatom, with ν^0 at 1013 cm^{-1} after anharmonicity correction, the anharmonicity constant is reported to be 4.9 cm^{-1} [39]. The higher anharmonicity of the V=O unit for surface vandia species relative to free V–O diatoms again suggests a mild vibrational coupling between the terminal V=O stretch and the other modes of the larger VO_4 unit.

4.2. Molecular structures of supported vanadia surface species during methanol oxidation

Exposure of the surface vanadium oxide species to the reaction stream of CH_3OH/O_2/He at different reaction temperatures produces two main changes in the metal–oxygen stretching region as observed by *in situ* Raman and IR spectroscopy: a decrease in intensity of the terminal V=O and bridging V–O–V Raman and IR bands, and a shift in the position of the V=O and V–O–V Raman and IR bands to lower wavenumbers. Furthermore, the decrease in intensity is similar for the surface vanadium oxide species on different oxide supports. These effects are more pronounced at lower reaction temperatures (100–230 °C) than at higher reaction temperatures (250–360 °C). The decrease in intensity and shift of the vibrational bands due to the V–O–V functionality is less pronounced since the band at 840–940 cm^{-1} is broad and changes are less evident. For V_2O_5/SiO_2, only one Raman band is present at 1033–1039 cm^{-1} that also shifts and decreases in intensity under the methanol oxidation reaction conditions. The *in situ* UV-Vis DRS spectra indicate a decrease in the surface V^{5+} LMCT band for vanadia on alumina, zirconia, and silica, while the weak d–d transition bands of reduced surface V^{3+}/V^{4+} species are detected only for surface vanadia on alumina and zirconia.

The decrease in intensities of bands associated with fully oxidized vanadia surface species in the Raman, IR, and UV-Vis DRS spectra under the methanol oxidation reaction conditions may be caused by two effects. Either a reduction in surface vanadia (V^{5+}) species to surface V^{3+}/V^{4+} species is occurring, or surface vanadia (V^{5+}) structural changes are induced by the chemisorption of CH_3OH reactant or H_2O product molecules on the surface vanadia sites. However, the reduction of surface vanadium (V^{5+}) oxide species to V^{3+}/V^{4+} species would be expected to increase with increasing temperature due to higher methanol conversion. Such behavior is not observed in the IR and Raman spectra, which instead clearly show that the decrease in band intensities is more pronounced at lower temperatures than at higher temperatures. The shift in vibrational frequency of the V=O band to lower wavenumbers is also consistent with a lengthening of the bond by coordination or H-bonding to adsorbed surface methoxy species or water, the former of which was directly detected by IR spectroscopy for all tested catalysts under methanol flow. While adsorbed water is generally displaced by methanol [32], the presence of a small amount of surface water species was also indicated by a broad IR band at $\sim$1615 cm^{-1} on alumina-supported catalysts at lower temperatures (not shown) and most likely contributes to the downshift in the V=O bands. Moreover, the UV-Vis DRS spectra exhibit a significantly greater intensity decrease in the surface V^{5+} LMCT band above 25,000 cm^{-1} for 1% V_2O_5/SiO_2 than for either of the other samples, yet no reduced surface V^{3+}/V^{4+} d–d transitions are detected in vanadia/silica (consistent with its very low activity [20]).

This behavior suggests that the V^{5+} LMCT band in UV-Vis DRS spectra and the V=O and V–O–V bands in the Raman and IR spectra are more significantly altered by coordination changes induced by chemisorbed methanol or water than by the surface vanadium cation reduction. A similar conclusion was recently reached by monitoring the V=O Raman band in the presence of water vapor over supported vanadia catalysts [13], and strong ligand effects were also recently observed in the UV-Vis DRS edge energies of dehydrated vanadia/silica catalysts [30]. The coordinating effects of such adsorbed surface species on the supported vanadia molecular structures are strongly dependent upon the concentrations of the adsorbed methoxy and water surface species. This is easily illustrated by comparing figures 5 and 8, where it is seen that the V=O distortions and surface methoxy concentrations are both highest at lower temperatures. An increase in temperature during steady-state flow reduces these concentrations by both lowering the equilibrium adsorption capacity (the dominant effect for surface methoxy concentration due to the generation of rapid steady-state adsorption equilibrium [32,33]) and by increasing the catalytic conversion of surface methoxy intermediates to oxidation and dehydration products. The partial pressure of methanol (or water) in the gas stream is also expected to influence the concentration of adsorbed methoxy intermediates, although the present results show that concentrations as low as 2000 ppm of methanol are already sufficient to induce significant changes in the V=O and V–O–V vibrations.

The above discussion demonstrates that it is very difficult or nearly impossible to use *in situ* Raman, IR, or UV-Vis DRS for monitoring of the surface vandia signals to quantify the number of vanadia sites participating in the

redox cycle during steady-state methanol oxidation. Essentially, most of the methanol-induced signal loss in the V=O, V–O–V, and V^{5+} LMCT bands associated with these fully oxidized vanadia structures is derived from H-bonding and other coordinating interactions between the vanadia surface sites and adsorbed methoxy or water surface species. Furthermore, the surface V^{5+} LMCT band also overlaps with the LMCT transitions from the reduced surface vanadia phases (indicated by the persistence of 40–90% of the original integrated area of this band even after H_2 reduction). In general, this means that the intensity losses in these bands during methanol oxidation are *not* simply representative of surface V^{5+} species lost to reduction in the redox cycle. A notable caveat is that for reactions like alkane oxidation, in which the rate-determining adsorption step is followed by rapid surface reaction [43], there is no appreciable concentration of surface intermediates for interaction with the unreduced surface vanadia sites and the complications associated with *in situ* quantification discussed above may not apply.

Boundaries on the maximum possible extent of reduction can, however, be estimated using the vibrational spectra at higher temperatures (300 °C in 4–6% methanol) or at lower methanol partial pressures (2000 ppm methanol at 230 °C), where the concentrations of surface methoxy species remain relatively low. This was presently done using the transmission IR data, which follow Beer's Law, by integrating the fundamental and overtone V=O bands for the monolayers of vanadia supported on TiO_2, CeO_2, ZrO_2, and Al_2O_2 (see baseline-corrected overtones of vanadia/alumina in the insert of figure 7(B)). The individual results are not given because they contain significant variations, sometimes even between overtone and fundamental bands for the same catalyst, due to the difficulty in integrating the long tails resulting from the methanol-induced downshifts in these bands. However, at 230 °C under 2000 ppm of methanol the percent vanadia reduction at steady-state generally ranged between 15 and 40%, and at 300 °C under 2000 ppm methanol this range narrowed to 15–25% vanadia reduction. This indicates that only a small fraction of surface vanadia sites are actually participating in the redox cycle at any given moment during steady-state methanol oxidation (i.e, the surface remains largely oxidized even during reaction). Nevertheless, all vanadia sites are still used for calculation of TOF values because each vanadium atom is capable of catalyzing methanol oxidation even though they do not all operate simultaneously.

More accurate or refined values for the percent surface vanadia reduction during steady-state methanol oxidation will require different techniques that monitor the reduced surface vanadia states directly. Unfortunately, the reduced states of surface vanadia species do not produce appreciable Raman or IR signals. This may be due to a lack of V=O terminal double bonds in the reduced phases, since the V=O vibration is the most distinctive feature in the fully oxidized surface vanadia phase. The weak d–d transitions at 10,000–30,000 cm^{-1} in the UV-Vis DRS spectra are also too weak to use quantitatively. Some success in quantifying the V^{4+} reduced phase has been achieved with electron paramagnetic resonance spectroscopy (EPR) [12,14,16]. However, additional progress will likely involve *in situ* (high temperature, atmospheric pressure) atomic spectroscopies that selectively monitor the surface vanadium cation oxidation state without significant influences from secondary ligand or coordination effects. In particular, Ruitenbeek et al. [44] have shown for several reactions that *in situ* X-ray absorption near-edge spectroscopy (XANES) can be used for this purpose with vanadia catalysts.

4.3. Detection of surface methoxy species during methanol oxidation

The results of the present study indicate distinct methoxy (–OCH_3) vibrations in the C–H stretching region (2800–3000 cm^{-1}) and in the C–O stretching/C–H bending region (1000–1600 cm^{-1}) of the IR and Raman spectra of supported vanadia catalysts during methanol oxidation. The assignments were given in section 3. These surface methoxy species were generally found to vibrate at different frequencies depending on the specific metal oxide upon which they chemisorb, and a slight shift to lower wavenumbers was observed at higher surface methoxy coverages (corresponding to lower temperatures) due to hydrogen-bonding between adjacent surface methoxy groups.

While adsorbed methoxy species were detected on all catalysts with IR spectroscopy, for the corresponding Raman spectra only silica, vanadia/silica, titania, and zirconia exhibited surface methoxy bands (methoxy bands on alumina and vanadia/alumina being obscured by fluorescence). For V_2O_5/TiO_2 catalysts, the intensity of the surface Ti–methoxy Raman bands at 2815, 2935, and 2965 cm^{-1} were seen to decrease with increasing vanadium oxide coverage until they completely disappeared at monolayer coverage (5% V_2O_5/TiO_2). This was expected because increasing the surface vanadium oxide coverage decreases the amount of exposed TiO_2 support, and, consequently, decreases the amount of Ti–methoxy species present. However, no new Raman bands were detected for the surface V–methoxy species despite their known presence from strong IR bands at 2832 and 2936 cm^{-1}. In the case of V_2O_5/SiO_2, new surface methoxy Raman bands were observed at 2830 and 2930 cm^{-1}, along with the surface methoxy bands due to the SiO_2 support at 2860 and 2960 cm^{-1}. The same surface methoxy bands were detected in the IR spectrum of vanadia/silica.

Considering only the intense methyl C–H modes, it is possible to have CH_3 point group symmetries of C_{3v}, C_s, and C_1, depending on the number of equivalent C–H bond lengths [39]. In C_{3v} symmetry there are four vibrations that are each Raman and IR active, while the six vibrations in the less symmetric C_s and C_1 point groups are also all active in both Raman and IR. Therefore, even though the actual surface selection rules may be somewhat different from these molecular selection rules, the failure to

detect surface methoxy bands in the Raman spectrum despite strong IR activity seems unlikely to be due to spectral inactivity associated with selection rules. Furthermore, the presence of significant steady-state surface methoxy concentrations as measured by IR indicates that the surface lifetime of these intermediates is sufficient for detection by the more energetic radiation employed by Raman.

Hence, the absence of detectable Raman surface methoxy bands in catalysts that exhibit significant IR surface methoxy bands can only be explained by low Raman scattering cross-sections (intensities). These Raman intensities depend in a complex way on the polarizability tensor of the adsorbed methoxy molecule and upon the fourth power of the incident light frequency [39]. It may be possible to observe some of the missing Raman bands by tuning the frequency of the incident light away from 514.5 nm. However, the sensitivity of the Raman scattering cross-sections of V–OCH_3 surface methoxy species to the underlying support oxide means that *in situ* IR spectroscopy is the superior technique for the detection of adsorbed methoxy intermediates during steady-state methanol oxidation. Additionally, while quantitative analysis is very difficult with Raman scattering, it is routinely performed with transmission IR spectroscopy through the use of Beer's Law [45].

5. Conclusions

In summary, the application of *in situ* Raman, IR, and UV-Vis DRS spectroscopies during steady-state methanol oxidation has demonstrated that surface vanadium oxide species supported on metal oxides are very sensitive to the coordination and H-bonding effects of adsorbed methoxy and water surface species. The coordination to surface vanadia species by these adsorbates, particularly the surface methoxy reaction intermediates, results in a decrease in the intensity of the spectral bands associated with the fully oxidized surface (V^{5+}) vanadia active phase. The intensity reductions occur in all three studied spectroscopies and are also accompanied by shifts in the terminal V=O and bridging V–O–V vibrational bands to lower frequency (e.g., the V=O band shifts from its fully oxidized frequency of $\sim$1030 cm^{-1} to as low as 1002 cm^{-1}). In the UV-Vis spectra, shifts to higher edge energies (V^{5+} LMCT band position at $>$25,000 cm^{-1}) also represent primarily ligand effects, since vanadia/silica experienced the greatest shift in edge energy but did not exhibit any bands from reduced V^{3+}/V^{4+} phases in the d–d transition region (10,000–30,000 cm^{-1}). Conversely, the vanadia/alumina and vanadia/zirconia catalysts experienced relatively small edge energy shifts, but were reduced to sufficient levels that the d–d transitions associated with reduced phases appeared in the spectra.

The magnitude of these ligand-based distortions also correlated with the concentrations of adsorbed methoxy intermediates and was most severe at lower temperatures and higher methanol partial pressures, where the surface methoxy concentrations were greatest. Conversely, spectral changes caused by actual reductions in surface vanadia (V^{5+}) species to reduced phases (V^{3+}/V^{4+}) would have been more severe at higher temperatures. These results further demonstrate that quantification of the number of surface vanadia sites simultaneously participating in the redox cycle during steady-state methanol oxidation cannot be performed based on the intensity reductions exhibited by the fully oxidized surface vanadia species. Some exception can be made using higher temperature (300 °C), lower methoxy surface coverage IR spectra, in which rough estimates suggest that the catalyst surfaces remain mostly oxidized during steady-state methanol oxidation (15–25% vanadia reduction).

However, a more reliable method for quantifying surface vanadia active sites will likely be the direct monitoring of the adsorbed surface methoxy intermediate species during methanol oxidation. These species were easily detected in the C–H stretching region (2800–3000 cm^{-1}) on all studied catalysts with *in situ* IR spectroscopy, and in transmission mode quantitative analysis can be made using Beer's Law (subject of future work). The methoxy species were generally found to vibrate at different frequencies depending on the specific metal oxide upon which they chemisorb, and a slight shift to lower wavenumbers was observed at higher methoxy coverages (low temperatures) due to hydrogen-bonding between adjacent methoxy groups. Interestingly, in the Raman spectra the surface methoxy vibrations were only detected on the silica, vanadia/silica, titania, and zirconia surfaces, with no V–OCH_3 bands being detected in the vanadia/titania or vanadia/zirconia catalysts. This phenomenon is attributed to a support-induced effect upon the electronic structure of the V–methoxy species that reduces the Raman scattering cross-sections (related to bond polarizabilities) in these catalysts. In general, however, *in situ* IR is a better method for the detection and quantification of adsorbed methoxy intermediates occupying the active vanadia surface sites during steady-state methanol oxidation.

Acknowledgement

The authors gratefully acknowledge the United States Department of Energy – Basic Energy Sciences (Grant #DEFG02-93ER14350) for financial support of this work.

References

[1] I.E. Wachs, Catal. Today 27 (1996) 437.
[2] J.M. Tatibouët, Appl. Catal. A 148 (1997) 213.
[3] I.E. Wachs, G. Deo, M.A. Vuurman, H. Hu, D.S. Kim and J.M. Jehng, J. Mol. Catal. 82 (1993) 443.
[4] P. Forzatti, E. Tronconi, A.S. Elmi and G. Busca, Appl. Catal. A 157 (1997) 387.
[5] (a) J.-M. Jehng and I.E. Wachs, J. Phys. Chem. 95 (1991) 7373;
(b) M.A. Vuurman and I.E. Wachs, J. Phys. Chem. 96 (1992) 5008.
[6] (a) D.S. Kim and I.E. Wachs, J. Catal. 142 (1993) 166;
(b) D.S. Kim and I.E. Wachs, J. Catal. 141 (1993) 419.

[7] Y. Matsuoka, M. Niwa and Y. Murakami, J. Phys. Chem. 94 (1990) 1477.
[8] (a) H. Hu and I.E. Wachs, J. Phys. Chem. 99 (1995) 10911.
(b) D.S. Kim, I.E. Wachs and K. Segawa, J. Catal. 146 (1994) 268.
[9] X. Gao and Q. Xin, J. Catal. 146 (1994) 306.
[10] Z. Sojka and M. Che, J. Phys. Chem. 99 (1995) 5418.
[11] (a) B.M. Weckhuysen and I.E. Wachs, J. Phys. Chem. B 101 (1997) 2793;
(b) B.M. Weckhuysen and I.E. Wachs, J. Phys. Chem. 100 (1996) 14437.
[12] (a) I.E. Wachs and B.M. Weckhuysen, Appl. Catal. A 157 (1997) 67;
(b) L.J. Burcham and I.E. Wachs, Catal. Today 49 (1999) 467.
[13] J.-M. Jehng, G. Deo, B.M. Weckhuysen and I.E. Wachs, J. Mol. Catal. A 110 (1996) 41.
[14] M.C. Paganini, L. Dall'Acqua, E. Giamello, L. Lietti, P. Forzatti and G. Busca, J. Catal. 166 (1997) 195.
[15] (a) N.-Y. Topsøe, H. Topsøe and J.A. Dumesic, J. Catal. 151 (1995) 226;
(b) N.-Y. Topsøe, J.A. Dumesic and H. Topsøe, J. Catal. 151 (1995) 241;
(c) N.-Y. Topsøe, J. Catal. 128 (1991) 499.
[16] S. Pak, C.E. Smith, M.P. Rosynek and J.H. Lunsford, J. Catal. 165 (1997) 73.
[17] (a) G.T. Went, S.T. Oyama and A.T. Bell, J. Phys. Chem. 94 (1990) 4240;
(b) A. Khodakov, B. Olthof, A.T. Bell and E. Iglesia, J. Catal. 181 (1999) 205;
(c) A. Khodakov, J. Yang, S. Su, E. Iglesia and A.T. Bell, J. Catal. 177 (1998) 343;
(d) G.T. Went, L.J. Leu, R.R. Rosin and A.T. Bell, J. Catal. 134 (1992) 492.
[18] K. Inumaru, M. Misono and T. Okuhara, Appl. Catal. A 149 (1997) 133.
[19] (a) F. Hatayama, T. Ohno, T. Maruoka, T. Ono and H. Miyata, J. Chem. Soc., Faraday Trans. 87 (1991) 2629;
(b) H. Miyata, M. Kohno, T. Ono, T. Ohno and F. Hatayama, J. Mol. Catal. 63 (1990) 181.
[20] (a) I.E. Wachs, G. Deo, M.V. Juskelis and B.M. Weckhuysen, in: *Dynamics of Surfaces and Reaction Kinetics in Heterogeneous Catalysis*, eds. G.F. Froment and K.C. Waugh (Elsevier, Amsterdam, 1997) pp. 305–314;
(b) I.E. Wachs, in: *Catalysis*, Vol. 13, ed. J.J. Spivey (The Royal Society of Chemistry, Cambridge, 1997) pp. 37–54.
[21] (a) G. Deo, I.E. Wachs and J. Haber, Crit. Rev. Surf. Chem. 4 (1994) 141;
(b) G. Deo and I.E. Wachs, J. Catal. 146 (1994) 323;
(c) G. Deo and I.E. Wachs, ACS Symp. Ser. 523 (1993) 31;
(d) G. Deo and I.E. Wachs, J. Catal. 129 (1991) 307.
[22] (a) S.C. Su and A.T. Bell, J. Phys. Chem. B 102 (1998) 7000;
(b) G.T. Went, L.J. Leu and A.T. Bell, J. Catal. 134 (1992) 479;
(c) G.T. Went, L.J. Leu, S.J. Lombardo and A.T. Bell, J. Phys. Chem. 96 (1992) 2235;
(d) S.T. Oyama, G.T. Went, K.B. Lewis, A.T. Bell and G.A. Somorjai, J. Phys. Chem. 93 (1989) 6786.
[23] F. Arena, F. Frusteri and A. Parmaliana, Appl. Catal. A 176 (1999) 189.
[24] N. Nag, K. Chary and V. Subrahmanyam, J. Chem. Soc., Chem. Commun. (1986) 1147.
[25] (a) U. Scharf, M. Schneider, A. Baiker and A. Wokaun, J. Catal. 149 (1994) 344;
(b) B.E. Handy, A. Baiker, M. Schraml-Marth and A. Wokaun, J. Catal. 133 (1992) 1;
(c) U. Scharf, M. Schraml-Marth, A. Wokaun and A. Baiker, J. Chem. Soc., Faraday Trans. 87 (1991) 3299;
(d) J. Kijenski, A. Baiker, M. Glinski, P. Dollenmeier and A. Wokaun, J. Catal. 101 (1986) 1.
[26] F. Roozeboom, P.D. Cordingley and P.J. Gellings, J. Catal. 68 (1981) 464.
[27] (a) C. Cristiani, P. Forzatti and G. Busca, J. Catal. 116 (1989) 586;
(b) I.E. Wachs, J. Catal. 124 (1990) 570;
(c) G. Ramis, C. Cristiani, P. Forzatti and G. Busca, J. Catal. 124 (1990) 574.
[28] F.D. Hardcastle and I.E. Wachs, J. Phys. Chem. 95 (1991) 5031.
[29] (a) L. Owens and H.H. Kung, J. Catal. 148 (1994) 587;
(b) L. Owens and H.H. Kung, J. Catal. 144 (1993) 202;
(c) P.J. Andersen and H.H. Kung, J. Phys. Chem. 96 (1992) 3114.
[30] X. Gao, S.R. Bare, B.M. Weckhuysen and I.E. Wachs, J. Phys. Chem. B 102 (1998) 10842.
[31] J.-M. Jehng, H. Hu, X. Gao and I.E. Wachs, Catal. Today 28 (1996) 335.
[32] G. Busca, A.S. Elmi and P. Forzatti, J. Phys. Chem. 91 (1987) 5263.
[33] W.L. Holstein and C.J. Machiels, J. Catal. 162 (1996) 118.
[34] (a) M.M. Ostromecki, L.J. Burcham, I.E. Wachs, N. Ramani and J. Ekerdt, J. Mol. Catal. A 132 (1998) 59;
(b) M.M. Ostromecki, L.J. Burcham and I.E. Wachs, J. Mol. Catal. A 132 (1998) 43.
[35] L.J. Burcham, Ph.D. dissertation, Lehigh University, Bethlehem, PA (1999).
[36] A.B.P. Lever, *Inorganic Electronic Spectroscopy* (Elsevier, Amsterdam, 1968).
[37] B.M. Weckhuysen and R.A. Schoonheydt, Catal. Today 49 (1999) 441.
[38] G. Busca, Catal. Today 27 (1996) 457.
[39] K. Nakamoto, *Infrared and Raman Spectra of Inorganic and Coordination Compounds*, 4th Ed. (Wiley, New York, 1986).
[40] J.H. Noggle, *Physical Chemistry*, 2nd Ed. (Harper Collins, New York, 1989).
[41] X. Gao and I.E. Wachs, unpublished results.
[42] (a) E. Ahlborn, E. Diemann and A. Müller, Z. Anorg. Allg. Chem. 394 (1972) 1;
(b) D.N. Sathyanarayana and C.C. Patel, Bull. Chem. Soc. Jpn. 37 (1964) 1736;
(c) B. Soptrajanov, A. Nikolovskii and I. Petrov, Spectrochim. Acta Part A 24A (1968) 1617.
[43] G. Busca, E. Finocchio, V. Lorenzelli, G. Ramis and M. Baldi, Catal. Today 49 (1999) 453.
[44] (a) M. Ruitenbeek, R.A. Overbeek, A.J. van Dillen, D.C. Koningsberger and J.W. Geus, Recl. Trav. Chim. Pays-Bas 115 (1996) 519;
(b) M. Ruitenbeek, Ph.D. Dissertation, Utrecht University, Utrecht (1999).
[45] A.T. Bell, in: *Vibrational Spectroscopy of Molecules on Surfaces*, eds. J.T. Yates and T.E. Madey (Plenum, New York, 1987) pp. 105–134.